RESEARCH ARTICLE

Differences in EEG Brain Activity for Black/White Versus RGB Stimuli

ALIREZA KHADIR[ID] **AND BORHAN BEIGZADEH**[ID]

Biomechatronics and Cognitive Engineering Research Laboratory, School of Mechanical Engineering, Iran University of Science and Technology, Tehran 16846-13114, Iran

Corresponding author: Borhan Beigzadeh (b_beigzadeh@iust.ac.ir)

ABSTRACT **Background:** Color perception is vital in many aspects of human behavior. It is tremendously engaged in the early stage of information processing to accelerate attention. Several studies focused on different aspects of the psychological effect of colors, which showed that color designs induce positive emotion, increased cognitive effort, and better learning outcomes compared to achromatic stimuli. Considering the importance of our daily encounters with colored stimuli, especially the RGB, black and white, studying the effect of these stimuli on brain activities is essential. **Method:** We investigated the significant differences in spatiotemporal brain activity of black, white, and RGB information. We used a task in which 12 participants were presented with random black-and-white and RGB-colored stimuli in a dark room. Each stimulus was displayed on the whole screen of a CRT calibrated monitor for 10 seconds. A 64-channel EEG device was used to acquire the EEG data. **Results:** Our results show that for RGB-colored stimuli, the beta power of the occipito-parietal region in early period (85 - 120 ms after stimulus onset) for RGB is higher than that of black ($p < 0.05$), while in late period (800 - 855 ms after stimulus onset), for RGB it is higher than that of both black and white ($p < 0.05$). Moreover, the alpha power of the centro-parietal region in late period (930 - 1360 ms after stimulus onset) for RGB is higher than that of black ($p < 0.01$). Finally, ITPC of alpha band in occipariatal region in the late period (840 - 920 ms after stimulus onset) for white is higher than black ($p < 0.05$) and RGB ($p < 0.01$). **Conclusion:** The results regarding brain responses to black/white and RGB stimuli, as well as beta and alpha-band differences in centro-pariatal and occipito-parietal regions provide valuable insights that can be interpreted within perception, emotional activities, and visual processes. Practical applications may span psychology, biofeedback, and BCI systems, with implications for cognitive training, rehabilitation, and human-computer interaction.

INDEX TERMS Color perception, EEG, alpha phase consistency, alpha and beta power.

I. INTRODUCTION

Color as a visual feature plays a vital role in many aspects of human behavior, and color perception is a fundamental cognitive feature of our psychological experience. Thus, human perception is considerably influenced psychologically and physiologically by the colors of the surrounding environment. Moreover, color is tremendously engaged in the early stage of information processing to accelerate attention [1].

The associate editor coordinating the review of this manuscript and approving it for publication was Siddhartha Bhattacharyya[ID].

Accordingly, compared to other visualization methods, color discrimination happens automatically in the pre-attention stage, which is relatively early [2], [3]. Furthermore, since colors also express semantic information, the accordance of color and the information it represents can boost easier and more accurate comprehension during the later phase of cognition [4], [5]. Visual information processing starts with light absorption. It is implemented by the three types of cone photoreceptors are short-, medium-, and long-wavelength. The spectral absorption functions of these cone cells are the base of human color vision [6].

Visual information is then sent to the cortex from retinal ganglion cells. The lateral geniculate nucleus (LGN), which consists of three separate cone-opponent channels, is the pathway by which the information transmits to the visual cortex [7]. The V1 and V2 areas of the brain are considered the first stage of cortical color processing, which involves registering the presence and intensity of different wavelengths. The V4 area, as the second stage, is preoccupied with automatic color constancy operations [8]. The third stage is more concerned with object colors and located on the inferior temporal, and frontal cortex [9].

In recent decades, numerous empirical works focused on different aspects of the psychological effect of colors [10], [11], [12], for example, colored multimedia learning [13], emotional effects [14], [15], [16], [17], [18], [19], [20], [21], memory facilitation, and cognitive performances. The results showed that compared to the neutral design (achromatic colors: grayscale, black and white), the colored design modulates a positive emotion, increased cognitive effort, and better learning outcomes. Others also reported that colored (red and blue) materials increased cognitive effort and caused positive emotion relative to achromatic materials [22]. Additionally, there are reports that neutral colors such as green boost calmness, in addition to the moderate, ordinary feelings, and warm colors in the red color system arouse warm, positive, active feelings. Subsequently, the cold, passive, quiet feelings are produced by the cool colors in the blue color system [23]. Saturated and bright colors were reported to cause significantly stronger skin conductance responses, indicating higher arousal levels [24]. Studies reported that compared to colors with shorter wavelengths (like blue), colors with longer wavelengths (like red) evoked a higher level of arousal emotion [25], [26], [27], [28].

On the other hand, the effects of colors on the neural activity of the brain are investigated with non-invasive methods in humans, such as Magnetoencephalography (MEG), functional-magnetic-resonance-imaging (fMRI), and Electroencephalography (EEG). For instance, Tcheslavski et al. [29] measured the EEG signals in response to continuously changing colors of the entire spectral range and found no inter-hemispheric asymmetry due to different intensities to specific hues. Moreover, the brain activity in response to red, white, and blue visual stimuli is examined with the fMRI technique [30]. Furthermore, it was found that blue stimulus inhibited the beta wave activity in the occipital areas, proposing the more relaxing effect of the blue [30]. Yoto et al. [23] used subjective emotional assessments and EEG and showed that red produces higher average power in theta and alpha rhythms in the frontal lobe. At the same time, in the emotional assessment, red also received more negative subjective scoring than blue and green. Therefore, it suggested that a higher level of brain activity due to the presentation of red is possibly elicited by an anxiety state for the subject.

To provide a better color design for improving the quality of our living environment, investigating the influence of colors including Red-Green-Blue (RGB), black and white on the human brain is necessary. Concerning the growth in daily usage of monitors and our life experiences and workspaces containing different colors, such study is inevitable. Although, the R, G, and B stimuli have deferent effects on brain response, finding similar effects of them is rarely studied in the literature. More important than this, there is no serious study to investigate the data-driven approach to find the deference between response mechanism of RGB vs black/white. In the present study, we investigated the brain response to the black, white, and RGB stimuli with studying the EEG signals. We used a task in which participants were presented with random black/white and RGB-colored stimuli. Here, we used data-driven approach to fill the gap by identifying spatial, spectral, and temporal brain patterns to discriminate between black/white and RGB colors. Our study demonstrated substantial differences in the power of beta and alpha-bands in the centro-parietal, and occipito-parietal regions, in addition to a significant phase coherency of alpha-band in the occipito-parietal area.

II. MATERIALS AND METHODS
The present study has been approved by the Iran University of Science and Technology and its ethics committee (ID number 95871) and was conducted in accordance with the declaration of Helsinki [31]. Meanwhile, before each test, subjects provided informed consent in accordance with the local ethics committee. All the applied procedures conform to the Declaration of Helsinki (1964) of the World Medical Association concerning human experimentation.

A. PARTICIPANTS AND SETUP
Participants in this and all subsequent experiments were naive to the experimental paradigm, had no previous neurological and psychiatric disorders, and reported normal or corrected-to-normal color vision. Participants were 3 female, 9 male in the age range of 20-28 years.

B. APPARATUS AND STIMULI
A CRT monitor with a resolution of 1024 × 768 pixels and a 60 Hz refresh rate was used in this experiment. The monitor's gamma and color calibration parameters were extracted using an X-Rite ColorMunki Display device (www.xrite.com) along with DisplayCAL software (www.displaycal.net). In particular, gamma correction values for RGB colors were cosidered to be $\gamma_R = 2.77$, $\gamma_G = 2.79$, and $\gamma_B = 2.76$, respectively. Participants sat in a dark room, isolated acoustically and electrically approximately 70 cm from the monitor.

Visual stimuli for this and all subsequent experiments were displayed on the whole screen. Black, white, and RGB colors were presented to the subject in each block, one at a time for 10 seconds aligned with previous related studies [74], [75], [76]. Moreover, RGB (here, red or green or blue) stimuli are isoluminance with $L = 8.99$ cd/m^2. The subject was shown a 3 seconds gray background as Inter-Trial interval (ITI) and

a 500 ms fixation point before each stimulus. Each subject completed the test five times.

C. EEG RECORDING AND PREPROCESSING

A 64-channel ANT neuro EEG signal acquisition device (ANT Neuro, Hengelo, The Netherlands) was used with a sampling rate of 512Hz. The electrodes used here were monopolar Ag/AgCl electrodes placed on scalp with a cap according to the standard 10-20 system. Figure 1 shows the positions of the electrodes. Two electrodes (A1 and A2) were connetcted to mastoide and their avereage was considered as reference; the ground was connected to FCz. The electrodes PO5 and PO6 were not used; finally, we employed the date gathered from remaining 59 channels.

The EEG pre-processing and processing was performed by custom-written Matlab scripts [32] and commands from the EEGLAB toolbox [33]. First, raw data were imported into MATLAB 2017b using ''pop_loadset()''. We applied a highpass filter at 0.1 Hz on EEG raw data by using ''eegfilt'' in the EEGLAB toolbox. Then, to extract epochs, the EEG signals were segmented from 1000 ms before to 2000 ms after stimulus onset followed by re-referencing the data to the average of the mastoids. It is worth noting that other alternatives for referencing method could be applied here such as the Reference Electrode Standardization Technique (REST) [34]; however, due to consistency with our ongoing studies and comparing to similar studies in the field utilizing linked-ear reference, and some technical considerations, we prefer using linked-ear reference method. To remove artifacts from the data, we used the Fully Automated Statistical Thresholding for EEG Artifact Rejection (FASTER) [35] algorithm, which uses a statistical threshold to reject bad channels and epochs. This algorithm uses five distinct statistical criteria to detect signals exhibiting anomalous behavior. These criteria encompass variance, correlation, the Hurst exponent, kurtosis, and susceptibility to line noise. A part of a channel and epoch is deemed aberrant with respect to a given criterion when its Z-score surpasses a threshold of 3 in that specific criterion. bad channels are reconstructed using the good channels with spherical spline interpolation which is implemented in the EEGLAB toolbox. To eliminate eye blinks and muscle activities, we first extracted the EEG components of each subject with the ''pop_runica'' EEGLAB command, then removed each of the noisy components with a visual inspection of the spectrum and topoplot. The whole procedure is depicted in Figure 2.

We combined all the RGB stimulus conditions and averaged them for further analysis. Therefore our final data was a 59 (electrodes) × 1792 (sample point) × 15 (3 conditions for black-white-RGB × 5 repetitions) matrix for each of the 12 subjects.

D. ERP, ERO AND TIME-FREQUENCY ANALYSIS

The EEG signal was bandpass filtered to capture only frequency-specific activity, with ''eegfilt()'' from EEGLAB Toolbox, which uses an order of $3 \times fix$(Fs/lowcutoff) zero-phase Finite Impulse Response (FIR) bandpass filter. Next, we applied a Hilbert Transform to obtain the bandpass data. The Hilbert transform extracts a complex signal from a signal that contains only a real part, and it can be represented using Euler's formula: $M(t)e^{i2\pi ft}$. The $M(t)$ is extracted as the instantaneous amplitude, and the following syntax is used to extract the complex analytic signal:

$$\text{hilbert(eegfilt(data, Fs, lowcutoff, highcutoff)')'} \quad (1)$$

where Fs is the sampling frequency (512 Hz), and we used delta (1-4 Hz), theta (4-8 Hz), alpha (8-12 Hz), beta (12-30 Hz), low gamma (30-50 Hz), and high gamma (70-150 Hz) for the lower and upper bound. For Event-Related Potential (ERP) analysis, we first applied a band-pass filter defined by cutoffs at 0.1 Hz and 30 Hz, exhibiting a roll-off rate of 12 dB/octave. For each trial, we applied such filtering using a second-order Butterworth filter implemented in MATLAB, and then used the mean() of all trials for extraction the ERP data for each subject. For grand-avaearge ERP, we take average of all subjects.

Event-Related Oscillations (ERO), like ERP analysis, provide insights into the temporal aspects of neural processing associated with cognitive tasks or sensory stimuli. In fact, ERO is the ERP that is applied in a specific frequency range whose measures can reflect different neurophysiological processes from ERP [36], [37], [38], [39]. For extracting ERO of each subject, the mean() of trials for each filtered frequency band was computed.

Inter-Trial Phase Clustering (ITPC) was used for the examination of cortical phase synchrony or for measuring the phase coherency over trials. ITPC measures the extent to which a distribution of phase angles at each time-frequency-electrode point across trials is nonuniformly distributed in polar space. The Mathematical representation of ITPC is as follows:

$$\text{ITPC}_{\text{tf}} = n^{-1} \sum_{r=1}^{n} e^{iK_{\text{tfr}}} \quad (2)$$

where n is the number of trials, e^{ik} is taken from Euler's formula and provides the complex polar representation of a phase angle k on trial r at time-frequency point tf. The syntax for computing the k is as follows:

$$\text{angle(hilbert(eegfilt((data, Fs, lowcutoff, highcutoff)'))} \quad (3)$$

ITPC is bounded by 0 and 1, with 0 indicating random phases and 1 indicating perfect phase coherency. In addition, because of the Gaussian shape of the frequency response of Morlet wavelets, wavelet convolution tends to produce smooth-looking and, therefore, easily visually interpretable time-frequency plots [40]. We performed a fine-grained complex Morlet wavelet convolution to the EEG epochs to analyze the data in the time-frequency domain with frequencies ranging from 2 to 80 Hz in 80 logarithmically spaced steps.
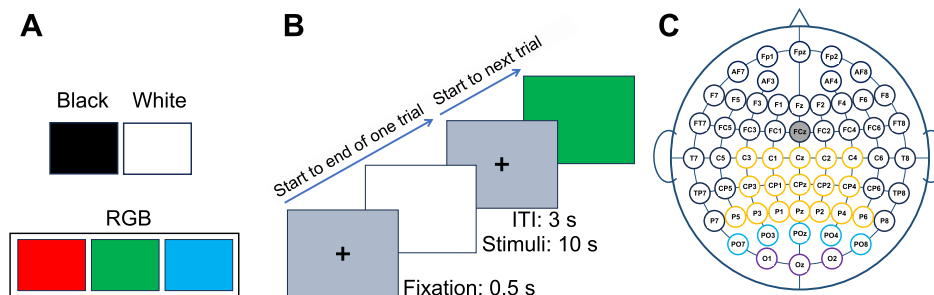
FIGURE 1. Stimulus characteristics, presentation, and electrode position A) Three types of color stimuli are used, which include white, black, and RGB colors. The RGB consists of the combination of red, blue, and green that all three are placed in the same category of RGB. B) The visual paradigm consists of 25 randomly selected stimuli, starting with a 0.5 s fixation point, after which participants were presented with a colored (black, white & RGB) screen for 10 s followed by a 3 s delay period. C) The location of the electrodes is based on the 10-20 system, and the areas marked on the electrodes are the regions mentioned in this article. The occipital area includes o1, oz, and o2 electrodes that are marked with a purple color. The occipito-parietal region includes O1, Oz, O2, PO3, PO4, POz, PO7, PO8 (purple and blue circles), and centro-parietal (P5, P3, P1, Pz, P2, P4, P6, CP3, Cp1, CPz, CP2, CP4, C3, C1, Cz, C2, C4) marked in orange.

E. TOPOGRAPHICAL MAPS

To illustrate the different ERO and time-frequency measures of the scalp distributions in each time window of interest, we created topographical maps using spline interpolation of the power and ITPC value differences between the orientations.

F. STATISTICAL ANALYSES

In order to compare the ERO for different pairs of colors, we employed statistical tests that do not rely on assumptions about the underlying distribution. Specifically, we utilized the two-sided Wilcoxon test at each time point. This test was chosen over the paired t-test because it is more suitable for situations where data violate assumptions of normality or involve small sample sizes. The Wilcoxon test provides a robust and flexible approach for comparing paired observations, particularly when parametric assumptions are not met. To conduct the analysis, we implemented a whole-subject permutation method, which offers a reliable and flexible approach for analyzing ERP data. Permutation tests accommodate the complex nature of ERP data, control for multiple comparisons, enable investigation of temporal effects, and are well-suited for small sample sizes. These tests are particularly advantageous for ERP analysis where distributional assumptions may not be met, and the focus is on capturing the temporal dynamics and characteristics of measured brain responses [41]. The whole-subject permutation method, an optimized and faster version of the permutation test, randomly inverted the sign of the ERO for each subject in each iteration [42]. By obtaining a distribution for each time point, we derived the P value of the null hypothesis.

To correct for multiple comparisons over time, we considered several alternatives such as False Discovery Rate (FDR), Bonferroni, and cluster-based methods. Among these, we opted for a cluster-based permutation analysis [43]. Cluster-based methods provide improved sensitivity, control over type I error, flexibility, and interpretability, making them

the preferred choice for multiple comparison correction in ERP analysis [41], [44]. In our study, we applied cluster-based permutation analysis with 1,000 permutations with significance level $p < 0.05$. We extended this method to compare ERO activity for multiple colors using a repeated-measures analysis of variance (rmANOVA). The same procedure was employed for analyzing power and ITPC values. To assess the statistical significance of the resulting time-frequency analysis, we repeated the aforementioned procedure for each time point and frequency.

Furthermore, to evaluate the statistical significance of Topographical maps, we employed the whole-subject permutation analysis with a two-sided Wilcoxon test. This analysis involved 59 electrodes with 5,000 permutations and a cluster-forming significance threshold of $p < 0.01$.

III. RESULTS

To demonstrate the response of the early visual sensory area to the stimulus presentation, neuronal EEG responses at occipital electrodes (O1, Oz, and O2) are shown in Figure 3. All color signals for each participant are integrated to extract the mean power, phase, and ERP of the data. The average time-frequency power of 12 participants produced by the Morlet Wavelets Convolution method, and based on Z-scored baseline normalization (300 - 100 ms prestimulus), is illustrated In Figure 3A. The plot shows a significant power increase under 10 Hz immediately after stimulus onset (permutation test with 1000 permutations, participant = 12, cluster-forming threshold $p < 0.01$, corrected significance level $p < 0.05$). Figure 3B demonstrated the average time-frequency plots of Z-scored p-values for ITPC of 12 subjects with the Morlet Wavelets Convolution method. To calculate the Z-scored values, first, the ITPC values from the baseline periods (100 - 300 ms prestimulus) are subtracted from each time-frequency point. The non-parametric Wilcoxon test and within-subject analysis are performed to extract Z-scored values. The highlighted cluster exhibits a
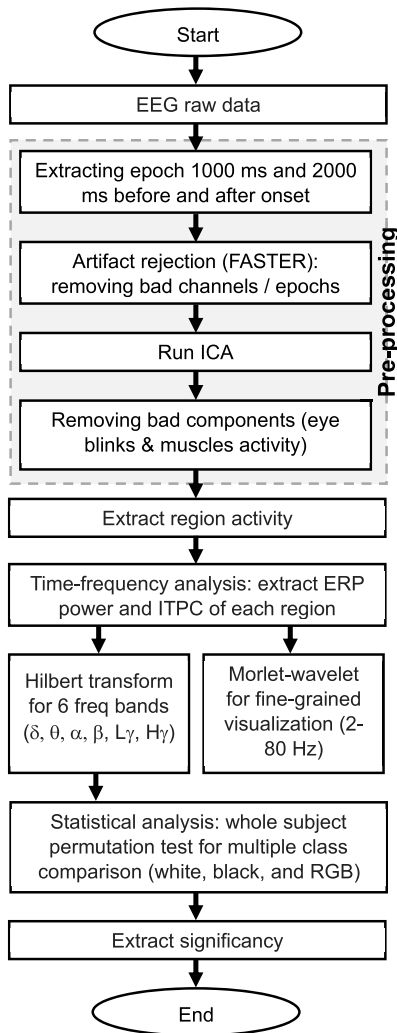
FIGURE 2. Flowchart of the procedure taken in the current study including pre-processing and analyses.

significant increase of under 10 Hz activity immediately after the stimulus presentation (permutation test with 1000 permutations, participant = 12, cluster-forming threshold $p < 0.01$, corrected significance level $p < 0.01$). Figure 3C shows an ERP below 30 Hz.

With data-driven approaches, we attempt to find the significant differences in the black, white, and RGB color information. To produce particular regions of interest, the resulting data of 59 electrodes were averaged (e.g., the mean value of O1, Oz, and O2 for the Occipital area). The ITPC values of each area are extracted with the Hilbert transform method in 6 band frequencies (delta, theta, alpha, beta, low gamma, high gamma). Then we applied the Wilcoxon signed-rank test to each time point for each pair of stimuli and inspected different brain areas and band frequencies for the meaningful significance for power and ITPC; see the Figure 2. Therefore, we found strong and reliable effects in the beta power of the occipito-parietal area and the alpha power of centro-parietal regions. In addition, we observed a

significant difference in the alpha ITPC value in the occipito-parietal electrodes. In Figure 4-6, we focused on these three spatial-frequency regions and applied an rmANOVA to compare the information in black/white vs. RGB colors.

We presented the average time-frequency power plots of 12 participants in the occipital (O1, Oz, and O2) electrodes for black (left), white (middle), and RGB (right) in Figure 4A. The power is extracted with Morlet Wavelets Convolution and based on Z-scored baseline normalization (300 - 100 ms prestimulus). As depicted, there is a significant power increase in late periods post-stimulus for RGB-colored stimuli (permutation test with 1000 permutations, participant = 12, cluster-forming threshold $p < 0.05$, corrected significance level $p < 0.05$). Although it is visible that for all three stimuli, the power increases immediately after the stimulus, this increase was not significant in the statistical analysis. Then, we focus on the beta band for comparison between stimuli. However, we must consider that in the power analysis of beta-band activity, we do not expect consistent behavior for a long period due to relatively high fluctuations.

Furthermore, Figure 4B-left shows the power average for black, white, and RGB color in beta-band frequency (12 - 30 Hz). It is evident that immediately after the stimulus onset, the power of white and RGB increases compared to the baseline, while black does not exhibit this level of power increase. The statistical analysis revealed a significant difference between colors in the early period (85 - 120 ms), and late period of 800 - 855 ms (within-subject rmANOVA, 1000 permutation, cluster-forming threshold $p < 0.05$, corrected significance threshold $p < 0.01$).

Figure 4B-right depicts the bar plot of averaged power values across the time window of significant periods in panel B-left side. The top view shows each color's averaged power (85 - 120 ms): black mean value -0.06 ± 0.23, white mean 1.17 ± 0.80, and RGB mean 0.96 ± 0.16. An rmANOVA found a significant difference between colors ($F(2,10) = 9.51$, $p < 0.005$). Post-hoc two-sided Wilcoxon tests showed a statistically significant difference between the RGB vs. black ($Z = 2.98$, $p < 0.003$). Accordingly, There was no significant effect on RGB vs. white or black vs. white. The bottom view shows the average power in (800 - 855 ms) of each color: black mean value -0.16 ± 0.24, white mean 0.10 ± 0.73, and RGB mean 0.46 ± 0.14. An rmANOVA found a significant difference between colors ($F(2,10) = 6.55$, $p < 0.02$). The Post-hoc two-sided Wilcoxon tests showed a statistically significant difference between the RGB vs. black ($Z = 2.66$, $p < 0.008$) and RGB vs. white ($Z = 2.03$, $p < 0.04$). There was no significant effect on black vs. white stimuli.

An important point that should be noted is the existence of high variability between subjects in response to white and black stimuli, which is less visible in response to RGB stimulus of beta-band activity. This effect is addressed in a separate article, which is under revision for publication. Considering that we illustrated a significant difference between the response of black vs. RGB color stimulus in
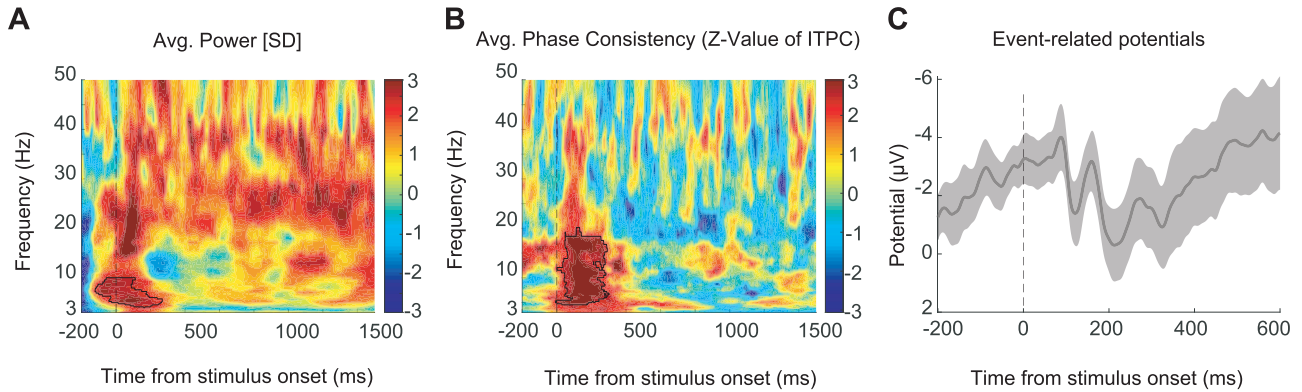
FIGURE 3. EEG Responses to Visual Stimuli in Occipital Region(O1, Oz, and O2) | A) Time-frequency power plots, averaged across color conditions (black, white, RGB), and Z-scored baseline normalization using the Morlet Wavelets Convolution method. Red indicates power exceeding baseline, blue signifies the opposite. Solid black outlines highlight significant clusters (permutation test with 1000 permutations, $n = 12$, cluster-forming threshold $p < 0.01$, corrected significance level $p < 0.05$). Dashed lines indicate stimulus onset ($t = 0$ ms). B) Z-scored p-values of ITPC values, similar to (A). C) Event-related potentials averaged across all color conditions.
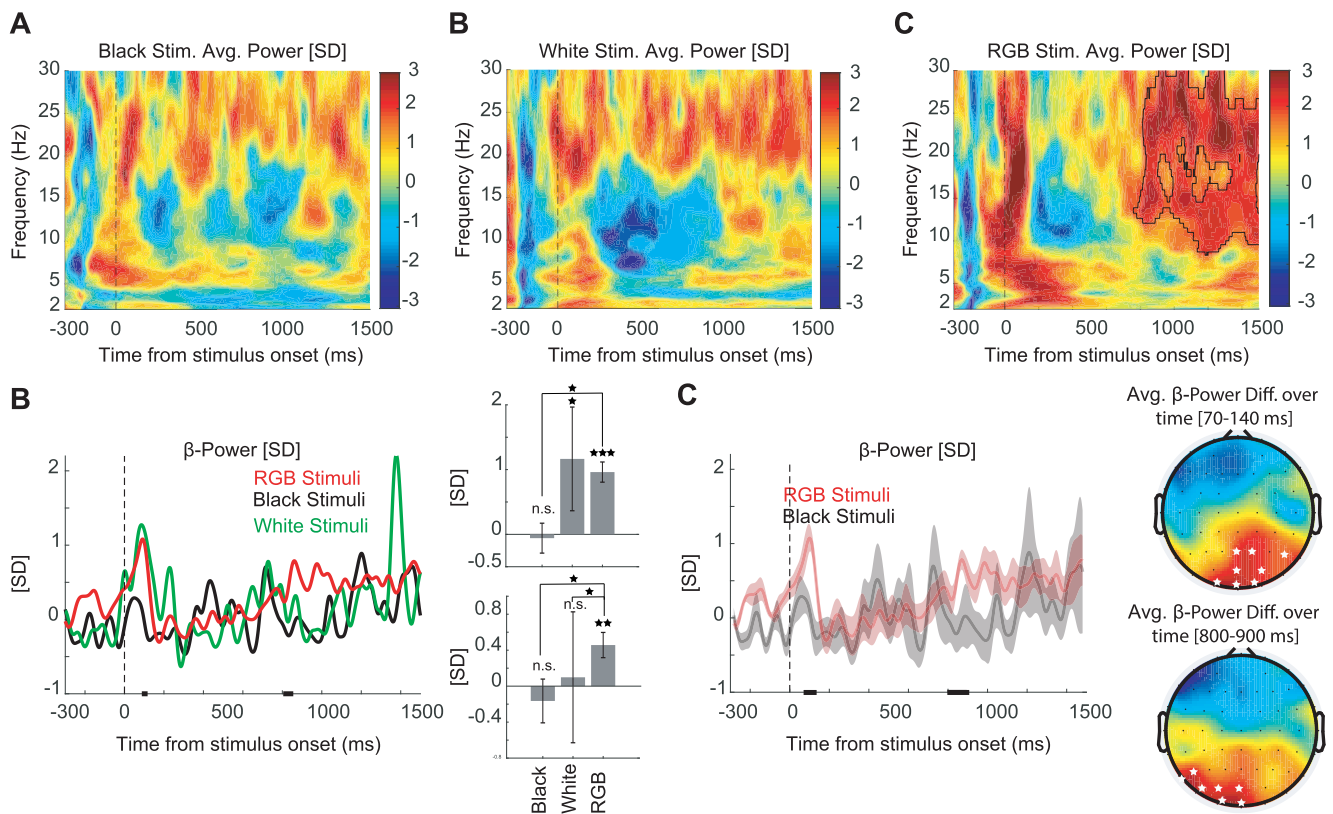

FIGURE 4. RGB power Information in Beta-band frequency of the occi-parietal (O1, Oz, O2, PO3, PO4, POz, PO7, PO8) electrodes | A) Time-frequency power plots for black, white, and RGB stimuli, focusing on frequencies under 30 Hz. Solid black outlines indicate significant clusters (permutation test with 1000 permutations, n = 12, cluster-forming threshold $p < 0.05$, corrected significance level $p < 0.05$) B) Left: Average power values in the beta band (12 - 30 Hz) reveal significant differences at 85 - 120 ms and 800 - 855 ms (within-subject rmANOVA, 1000 permutations, $n = 12$, cluster-forming threshold $p < 0.05$, corrected significance threshold $p < 0.01$). Right: Bar plots illustrate these power differences with error bars representing 95% confidence intervals across 12 participants. Asterisks denote significance from zero (Wilcoxon rank sum test), and asterisks above horizontal lines indicate significant differences between color pairs (Post-hoc two-sided Wilcoxon tests). n.s: $p > 0.05$, *$p < 0.05$, **$p < 0.01$, ***$p < 0.001$. C) Left: Average power values for black and RGB colors, similar to (B-left), with horizontal lines indicating clusters of significant differences (two-sided Wilcoxon tests, 1000 permutations, cluster-forming threshold $Z > 1.96$, corrected significance threshold $p < 0.05$). Right: Topographies depict differences between black and RGB colors in the beta band during the 70 - 140 ms and 800 - 900 ms time windows. Stars indicate significant sites (5000 permutations, cluster-forming threshold $Z > 2.35$, corrected significance threshold $p < 0.005$).

panel B-right; therefore, in panel C, we focused on the analysis between these two colors for scalp EEG distribution (Figure 4C).

Figure 4C-left shows the power values of black and RGB colors. There are meaningful differences in a time window of 70 - 140 ms and 800 - 900 ms (two-sided Wilcoxon
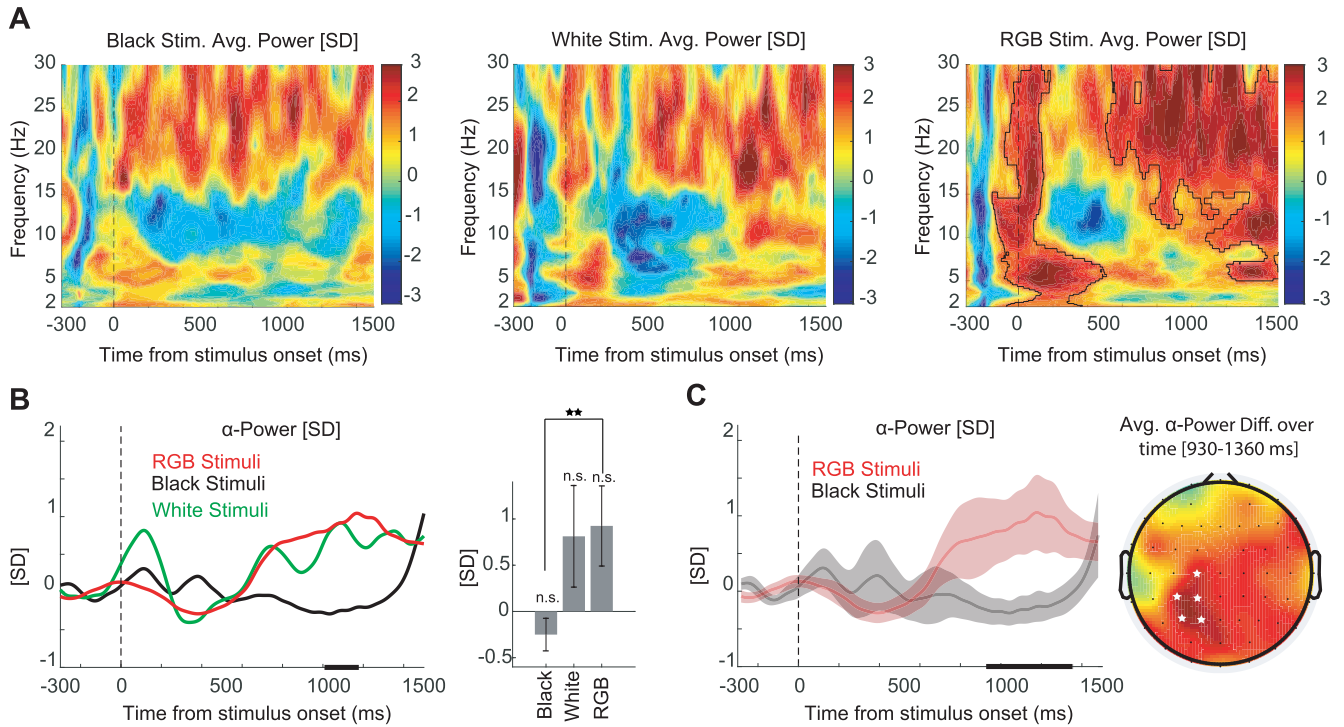
FIGURE 5. Color power information in alpha-band frequency of the centro-parietal (P5, P3, P1, Pz, P2, P4, P6, CP3, Cp1, CPz, CP2, CP4, C3, C1, Cz, C2, C4) electrodes | A) Time-frequency power plots for black, white, and RGB stimuli, focusing on frequencies under 30 Hz. Solid black outlines indicate significant clusters (permutation test with 1000 permutations, $n = 12$, cluster-forming threshold $p < 0.05$, corrected significance level $p < 0.05$). B) Left: Average power values in the alpha band (8- 12Hz) show the clusters of significant differences in the time window of 1000 - 1180 ms (within-subject rmANOVA, 1000 permutations, $n = 12$, cluster-forming threshold $p < 0.05$, corrected significance threshold $p < 0.05$). Right: Bar plots illustrate these power differences with error bars representing 95% confidence intervals across participants. Asterisks denote significance from zero (Wilcoxon rank sum test), and asterisks above horizontal lines indicate significant differences between color pairs (Post-hoc two-sided Wilcoxon tests). n.s: $p > 0.05$, *$p < 0.05$, **$p < 0.01$, ***$p < 0.001$. C) Left: Average power values for black and RGB colors, similar to (B-left), with horizontal lines indicating a cluster of significant differences (two-sided Wilcoxon tests, 1000 permutations, cluster-forming threshold $Z > 1.96$, corrected significance threshold $p < 0.05$). Right: Topographies depict differences between black and RGB colors in the alpha band during the 930- 1360 ms time windows. Stars indicate significant sites (5000 permutations, cluster-forming threshold $Z > 2.51$, corrected significance threshold $p < 0.005$).

tests,1000 permutations, cluster-forming threshold $Z > 1.96$, the corrected significance threshold $p < 0.05$). Figure 4C-right demonstrates the topoplot of Z-valued for the two-sided Wilcoxon test for black and RGB in theta-band power at 70 - 140 ms (top) and 800 - 900 ms (bottom) after the stimulus onset. Subsequently, the statistical analysis indicates significant sites in top: O1-Oz-POz-P2-Pz-P8-O2-PO4, and bottom: Oz-O1-PO7-P5-P7-POz-PO3 (5000 permutations, cluster-forming threshold $Z > 2.35$, corrected significance threshold $p < 0.005$).

Figure 5A shows the time-frequency average of power plots extracted with Morlet Wavelets and based on Z-scored baseline normalization (300-100 ms time-window before stimulus onset) for 12 participants in the centro-parietal (P5, P3, P1, Pz, P2, P6, CP3, Cp1, CPz, CP2, CP4, C3, C1, Cz, C2, C4) electrodes for black(left), white(middle) and RGB(right). Although the plot for all three stimuli illustrated an evident increase in the power of beta immediately after the stimulus, in the statistical analysis, this increase is only significant in late periods for RGB stimuli (permutation test with 1000 permutations, participant = 12, cluster-forming threshold $p < 0.05$, corrected significance level $p < 0.05$).

However, there was no significant difference between the stimuli (RGB vs. black, RGB vs. white, and black vs. white) for the beta band. On the other hand, it can be seen that in all three stimuli, alpha has been suppressed after 200 ms post-stimulus onset, and this suppression for black color happens in late periods and continues for a longer duration, while for white and RGB color it only lasts shorter. The statistical analysis showed this suppression was insignificant in any stimuli. However, a significant difference can be seen in the comparison between the stimuli analyzed in panels B and C.

The average power of alpha-band frequency (8-12 Hz) for black, white, and RGB color is shown in Figure 5B-left. The power of the black color has decreased compared to baseline activity in late periods. At the same time, an increase is observed in the white and RGB color. There is a significant difference between colors in the 1000 - 1180 ms (within-subject rmANOVA, permutation test with 1000 permutations, participant = 12, cluster-forming threshold $p < 0.05$, corrected significance level $p < 0.05$). Figure 5B-right depicts the bar plot of averaged power values across the time window of significant periods in panel B-left. The averaged power of each color: black mean value -0.25 ± 0.18, white

mean 0.81 ± 0.55, and RGB mean 0.93 ± 0.43. An rmANOVA showed a significant difference between colors (F(2,10) = 5.34, $p < 0.03$). Post-hoc two-sided Wilcoxon tests showed a statistically significant difference between the black vs. RGB ($Z = 2.74$, $p < 0.007$). There was no significant effect on RGB vs. white or black vs. white. Considering that in the right panel B, we showed a significant difference between the response to the black and the RGB stimulus; therefore, in panel C for the scalp EEG distribution, we focused on the analysis between these two colors. (Figure 5C).

Figure 5C-left shows the power values of black and RGB colors. There is a significant difference in a time window of 930 - 1360 ms (two-sided Wilcoxon tests,1000 permutations, cluster-forming threshold $Z > 1.96$, the corrected significance threshold $p < 0.05$). Figure 5C-right shows the topoplot of the Z-valued of the two-sided Wilcoxon test for black and RGB in alpha-band power at 930 - 1360 ms post-stimulus onset. The statistical analysis indicates that centro-parietal regions (P1-P3-Cp1-Cp3-C1) are significant sites (5000 permutations, cluster-forming threshold $Z > 2.51$, corrected significance threshold $p < 0.005$).

We performed an exploratory analysis of different areas over 6 frequency bands to find the information difference in phase consistency analysis. We reached a remarkable result in the occipito-parietal (O1, Oz, O2, PO3, PO4, POz, PO7, PO8, P7, P5, P3, P1, Pz, P2, P6, P8) region in the alpha frequency band (Figure 6). Figure 6A demonstrates the average time-frequency plots of within-subject Z-scored value for ITPC values of 12 participants (blue(left), green(middle), and red(right)). To extract time-frequency values similar to the previous analysis, we used the Morlet Wavelets Convolution method. Each time-frequency point was subtracted from baseline periods (300 - 100 ms before stimulus onset). As can be seen, the ITPC values increased for all three stimuli immediately after the stimulus onset for frequencies below 30 Hz and particularly below 15 Hz. However, this increase was only significant in RGB stimuli (permutation test with 1000 permutations, participant = 12, cluster-forming threshold $p < 0.05$, corrected significance level $p < 0.05$). Subsequently, this effect is not significant in the comparison between stimuli. It is also evident that the ITPC values in the alpha band in the late periods have decreased for the RGB stimuli while it has increased for the white stimulus. Yet, the black stimulus exhibits neither an increase nor a decrease. Although this observation was not significant in the statistical analysis for each stimulus, however, in comparison between stimuli, the ITPC values for the alpha band differ significantly, as discussed in panels B and C.

In Figure 6B-left, each line shows the ITPC average for each color in alpha-band frequency (8-12 Hz). It is evident that there is no substantial difference in the first 500 ms post-stimulus onset. However, after 500 ms, the ITPC value decreases for RGB and black stimuli, while it increases for white. The within-subject rmANOVA statistical analysis showed a considerable difference between colors in the time window of 840 - 920 ms (permutation test with $n = 1000$,

cluster-forming threshold $p < 0.005$, corrected significance threshold $p < 0.05$). Figure 6B-right indicates the bar plot of averaged ITPC values across the time window of significant periods in panel B-left (840 - 920 ms). The ITPC mean values are as follows: black mean value -0.02 ± 0.05, white mean value 0.15 ± 0.05, and RGB's mean value -0.09 ± 0.04. There was a meaningful difference between colors (an rmANOVA, F(2,10) = 17.97, $p < 0.0004$). Post-hoc two-sided Wilcoxon tests showed a statistically significant difference between the black vs. white ($Z = 2.43$, $p < 0.02$) and white vs. RGB ($Z = 2.98$, $p < 0.002$). There was no significant effect on RGB vs. black. As can be seen, the averages of white and RGB are substantial compared to zero and also have a strong significant difference from each other, therefore, in panel C, we focused only on these two stimuli to check the Scalp distribution for ITPC values.

Figure 6C-left shows the alpha ITPC values of white and RGB colors. We observed a significant difference in a time window of 800 - 970 ms (two-sided Wilcoxon tests, 1000 permutations, cluster-forming threshold $Z > 2.2$, the corrected significance threshold $p < 0.05$). In Figure 6C-right, the topoplots for the Z-value of two-sided Wilcoxon of white vs. RGB in alpha ITPC are illustrated (at 800 - 970 ms after the stimulus onset). The P6-P4-PO4-CP6-CP4-Oz-P2-PO8-Pz-CPz-P8-POz-P1-O2-P3-CP2-CP1-PO3 electrodes are significant sites (5000 permutations, cluster-forming threshold $Z > 2.19$, corrected significance threshold $p < 0.01$).

IV. DISCUSSION

Considering the importance of our daily encounters with colored stimuli, especially the RGB, black and white, studying the effect of these stimuli on brain activities is essential. While previous studies have explored the effects of color on brain responses, the majority of them have primarily focused on comparing different color stimuli [77], [78], [79], [80] or black vs white [81] without specifically investigating the differences between black and white and RGB stimuli. However, in our everyday experiences, when individuals try to describe the color of an object, they often use general categories such as a ''white object'', a ''black object'', or a ''colored object''. While color is distinctly different from black and white, it doesn't imply that black and white fall into the same category. By directly comparing these three stimulus types (black, white, and RGB), our study provides novel insights into the distinctive neural mechanisms underlying color processing. The data-driven approach we employed allowed us to identify discriminative features that highlight the response patterns associated with black/white and RGB stimuli. Our results showed significant differences in color data information of black/white vs. stimuli in the occipital, parietal, and centro-parietal regions in the alpha and beta bands. Nevertheless, it is believed that compared to achromatic colors, colored stimuli modulate positive emotion and influence cognitive effort. Therefore, these results can be interpreted in the form of emotionality of color stimuli compared to black and white. These findings
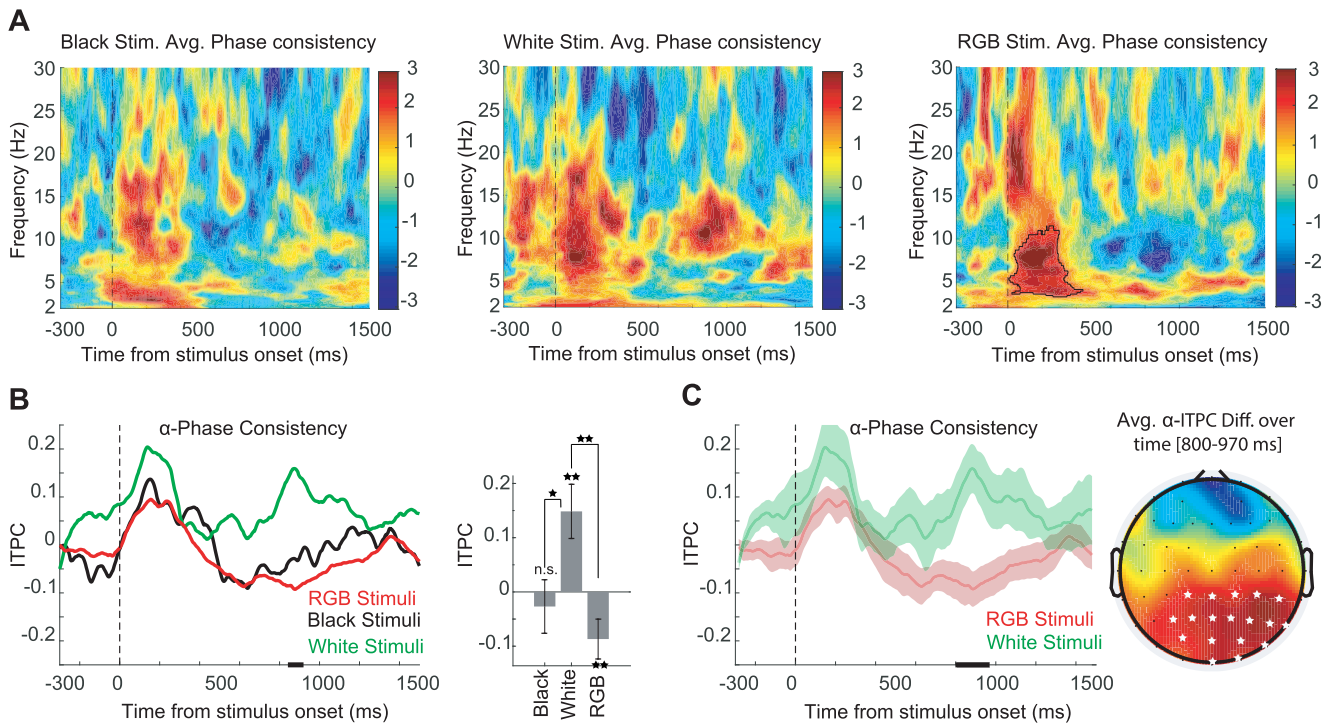
FIGURE 6. Color phase information in alpha-band frequency in occi-parietal (O1, Oz, O2, PO3, PO4, POz, PO7, PO8,P7, P5, P3, P1, Pz, P2, P6, P8) electrodes | A) Time-frequency Z-scored p-values for ITPC for black, white, and RGB stimuli, focusing on frequencies under 30 Hz. Solid black outlines indicate significant clusters (permutation test with 1000 permutations, $n = 12$, cluster-forming threshold $p < 0.05$, corrected significance level $p < 0.05$). B) Left: Average ITPC values (Z-scored p-values) in the alpha band (8- 12Hz) show the clusters of significant differences in the time window of 840- 920 ms (within-subject rmANOVA, 1000 permutations, $n = 12$, cluster-forming threshold $p < 0.005$, corrected significance threshold $p < 0.05$). Right: Bar plots illustrate these ITPC differences with error bars representing 95% confidence intervals across participants. Asterisks denote significance from zero (Wilcoxon rank sum test), and asterisks above horizontal lines indicate significant differences between color pairs (Post-hoc two-sided Wilcoxon tests). n.s: $p > 0.05$, *$p < 0.05$, **$p < 0.01$, ***$p < 0.001$. C) Left: Average ITPC values for white and RGB colors, similar to (B-left), with horizontal lines indicating a cluster of significant differences (two-sided Wilcoxon tests, 1000 permutations, cluster-forming threshold $Z > 2.2$, corrected significance threshold $p < 0.05$). Right: Topographies depict differences between white and RGB colors in the alpha band during the 800 - 970 ms time windows. Stars indicate significant sites (5000 permutations, cluster-forming threshold $Z > 2.19$, corrected significance threshold $p < 0.01$).

contribute to the existing literature by addressing a significant research gap and offer a new perspective on the neural processes involved in color perception.

The beta power of RGB colors relative to the baseline activity is significantly higher than black colors. There are different reports of beta oscillation related to the brain's emotional activity. Some authors reported that beta oscillations reflect emotional processes and found that the presentation of pleasant stimuli increased beta activity in temporal and parietal areas [45]. In contrast, a study showed that the pleasant stimuli compared to neutral stimuli, induced higher beta responses only at the occipital recording sites [46]. Furthermore, the beta oscillatory response was also found to be high during anxiety [47] or in response to anxious rumination [48]. However, the results of mentioned studies indicate different effects on beta responses produced by different types of stimuli and showed that emotionally significant pictures could elicit a higher beta response in the occipital region. Considering the literature reports that compared the neutral design (achromatic colors: grayscale, black and white), and colored design that modulates a positive emotion, increased cognitive effort, and better learning

outcomes [22]. We concluded that the observed significant difference in occipital electrodes in beta-band power is due to the different emotional modulation of RGB and achromatic colors on the brain.

Other important findings of the present study revealed a significant effect in the alpha-band power analysis, which brings us to the available evidence on the role of alpha activity in various emotional and cognitive processes of the brain. The occipital alpha band activity is seen predominantly at the time of awakening, generally appearing primarily in a state of relaxation [23]. Additionally, in the cognitive domain (i.e., perception, attention, working memory), researchers reported a decrease in alpha power in brain regions activated during a cognitive task [49], [50], [51]. Evidence also shows decreases in alpha power that may reflect cortical activation induced by emotional stimulation [52], [53]. In the context of emotional processes, however, findings are difficult to integrate because they vary considerably due to variations in the choice of stimulation, task instructions, time windows, and topographies. Some authors reported an increase in alpha power for emotionally significant stimuli [54], [55], [56]. Moreover, based on the cognitive literature, Event-Related

Synchronization (ERS) of alpha might be involved in emotional modulations of perception and attention. Thus, it reported that the correlation of alpha power with emotional arousal is due to increased neural inhibition induced by affective attention [56]. In contrast, some studies reported alpha-band desynchronized brain oscillations elicited by emotional stimuli [57], [58], [59], [60], [61], [62], [63], [64]. However, the result of our study showed that in contrast to white and RGB colors, black-colored stimulus produces a negative alpha power value relative to baseline activity in the certro-parietal regions. With an emphasis on the emotional and psychological aspects of color perception, we suggest that RGB colors and white stimuli probably produce more emotional arousal than black, which may result in our observed alpha behavior.

It has been proposed that phase coherence represents a mechanism to optimize data processing by regulating the brain's response to the temporal configuration of task-related information [65], [66], [67], [68]. The higher degree of phase locking or consistency of the phase with the timing of stimulus presentation across trials is reported to be associated with attention [69], [70] and visual perception [71]. The present study found that the alpha-band ITPC value of white-colored stimulus increased considerably at 800 - 1000 ms after stimulus onset. We suggest that this increase in alpha-band phase coherence may be interpreted as the result of extra attention or visual perception processes that particular colors (e.g., white) modulate in the brain. Furthermore, the color information could be transmitted through phase synchronization of different areas associated with these processes.

V. CONCLUSION: APPLICATIONS, LIMITATIONS, AND FUTURE WORKS

The findings of this study regarding the differential brain responses to black/white stimuli and RGB stimuli have important implications for our understanding of visual perception and the underlying neural mechanisms involved. By employing a data-driven approach, we were able to identify distinctive features that effectively discriminate between these stimuli. This knowledge contributes to the existing literature by addressing a significant research gap in understanding how the brain processes and differentiates between various types of visual stimuli. This resulted in substantial differences in the power of beta and alpha-bands, which are known to associate with emotional modulations of perception, attention, and visual processes. Moreover, the transmission of color information during the presentation of black and white vs. RGB stimuli may correlate with different degrees of alpha-band phase locking through occipito-parietal regions of the brain.

The practical implications of these findings extend beyond the realm of neuroscience, with potential applications in fields such as psychology including psychological assessments and diagnostic tools. By understanding the specific neural mechanisms associated with these stimuli, it may be

possible to develop more sensitive and precise psychological assessments that utilize color stimuli [13], [23], [82], [83], [84], [85]. This could be particularly relevant in areas such as visual psychophysics, where color perception plays a critical role. In addition, the study's findings have practical implications for fields such as industrial and environmental psychology [86], [87]. Understanding how different types of stimuli impact brain responses can inform the design of visual displays, user interfaces, and environmental settings to optimize human perception, attention, and well-being. By considering the specific effects of black/white and RGB stimuli, psychologists can provide evidence-based recommendations for creating visually stimulating and engaging environments. Another interesting relevant application is neuromarketing which has been explored in recent studies [88].

Furthermore, it is important to highlight the potential practical implications of understanding the response mechanisms of black, white, and RGB stimuli. By gaining a deeper understanding of how the brain processes these stimuli, we can explore their applications in biofeedback or brain-computer interface (BCI) systems. If we can discern the specific response mechanisms associated with black, white, and RGB stimuli, it opens up the possibility of utilizing them in these systems to control the power and phase consistency of brain activity. This knowledge could facilitate the development of more effective and precise techniques for utilizing visual stimuli in neurofeedback paradigms or BCI applications, ultimately leading to advancements in cognitive training, rehabilitation, and human-computer interaction. Therefore, our study not only contributes to fundamental research on color perception but also holds promising implications for practical applications in the field of BCI systems. For instance, in the context of BCI and Steady-State Visually Evoked Potentials (SSVEP), numerous studies have explored the impact of color stimulus selection on SSVEP accuracy, response time, Information Transfer Rate (ITR), and other performance metrics. These studies have highlighted the significance of color choice in optimizing SSVEP-based BCI systems [72], [73]. By investigating the effects of different colors and frequencies on the Signal-to-Noise Ratio (SNR) of SSVEP responses, our study contributes valuable complementary insights to the existing research in this field. Specifically, our findings shed light on the suitability of various colors in SSVEP paradigms and can inform the selection of optimal colors for achieving enhanced performance and usability in SSVEP-based BCI applications.

The current study has several limitations that should be acknowledged. Firstly, the use of a darkroom for EEG signal acquisition may have influenced the participants' visual experience and could potentially impact the generalizability of the results to real-world settings. Additionally, the study employed a limited number of isoluminant colors, which may not fully capture the complexity and variability of natural color stimuli. Furthermore, the sample size of the study was relatively small, consisting of 12 participants; increasing the number of participants would enhance the statistical power

and generalizability of the findings. Furthermore, the other limitation of this study is the failure to record and evaluate the rate of the emotional valence of the color stimuli by the participants. Lastly, we acknowledge the gender imbalance in our participant pool due to the number of female participants (3 females) compared to the number of male participants (9 males). This matter is still open to further investigation in future works. It is important to consider these limitations when interpreting the results. Future research should aim to address these limitations by conducting similar studies in more ecologically valid settings, using a broader range of colors in RGB, CIELAB, and Derrington-Krauskopf-Lennie (DKL) color spaces, increasing the sample size to enhance the robustness and applicability of the findings, and quantifying and finding the correlation between subjects' emotional valence responses and brain signals. By overcoming these limitations, future works can provide a more comprehensive understanding of the brain's response to color stimuli and further advance our knowledge in this field.

ACKNOWLEDGMENT

REFERENCES

[1] M. Friedrich and M. Vollrath, "Urgency-based color coding to support visual search in displays for supervisory control of multiple unmanned aircraft systems," *Displays*, vol. 74, Sep. 2022, Art. no. 102185, doi: 10.1016/j.displa.2022.102185.

[2] A. Treisman, "Preattentive processing in vision," *Comput. Vis., Graph., Image Process.*, vol. 31, no. 2, pp. 156–177, 1985.

[3] M. Yeh and C. D. Wickens, "Attentional filtering in the design of electronic map displays: A comparison of color coding, intensity coding, and decluttering techniques," *Hum. Factors*, vol. 43, no. 4, pp. 543–562, 2001, doi: 10.1518/001872001775870359.

[4] M. L. Larrea, S. Martig, and S. M. Castro, "Semantics-based color assignment in visualization," *J. Comput. Sci. Technol.*, vol. 10, pp. 14–18, Jan. 2010.

[5] S. C. Sibrel, R. Rathore, L. Lessard, and K. B. Schloss, "The relation between color and spatial structure for interpreting colormap data visualizations," *J. Vis.*, vol. 20, no. 12, pp. 1–20, 2020, doi: 10.1167/jov.20.12.7.

[6] H. Sun, H. E. Smithson, Q. Zaidi, and B. B. Lee, "Specificity of cone inputs to macaque retinal ganglion cells," *J. Neurophysiol.*, vol. 95, no. 2, pp. 837–849, Feb. 2006.

[7] K. R. Gegenfurtner and D. C. Kiper, "Color vision," *Annu. Rev. Neurosci.*, vol. 26, no. 1, pp. 181–206, 2003.

[8] S. Zeki and A. Bartels, "The clinical and functional measurement of cortical (in)activity in the visual brain, with special reference to the two subdivisions (V4 and V4α) of the human colour centre," *Philos. Trans. Roy. Soc. London. B, Biol. Sci.*, vol. 354, no. 1387, pp. 1371–1382, 1999.

[9] S. Zeki and L. Marini, "Three cortical stages of colour processing in the human brain," *Brain: J. Neurol.*, vol. 121, no. 9, pp. 1669–1685, 1998.

[10] N. Abbas, D. Kumar, and N. Mclachlan, "The psychological and physiological effects of light and colour on space users," in *Proc. IEEE Eng. Med. Biol. 27th Annu. Conf.*, Shanghai, China, Jan. 2006, pp. 1228–1231, doi: 10.1109/IEMBS.2005.1616646.

[11] P. Anjana, S. Bavatarani, and D. Kumar, "A study on human behavior based color psychology using K-means clustering," in *Proc. Int. Conf. Inventive Comput. Technol. (ICICT)*, Feb. 2020, pp. 608–612.

[12] G. M. Murch, "Physiological principles for the effective use of color," *IEEE Comput. Graph. Appl.*, vol. CGA-4, no. 11, pp. 48–55, Nov. 1984, doi: 10.1109/MCG.1984.6429356.

[13] M. T. Chai, H. U. Amin, L. I. Izhar, M. N. M. Saad, M. Abdul Rahman, A. S. Malik, and T. B. Tang, "Exploring EEG effective connectivity network in estimating influence of color on emotion and memory," *Frontiers Neuroinform.*, vol. 13, p. 66, Oct. 2019. [Online]. Available: https://www.frontiersin.org/articles/10.3389/fninf.2019.00066/full, doi: 10.3389/fninf.2019.00066.

[14] F. M. Adams and C. E. Osgood, "A cross-cultural study of the affective meanings of color," *J. Cross-Cultural Psychol.*, vol. 4, no. 2, pp. 135–156, 1973.

[15] W. Wei-Ning, Y. Ying-Lin, and J. Sheng-Ming, "Image retrieval by emotional semantics: A study of emotional space and feature extraction," in *Proc. IEEE Int. Conf. Syst., Man Cybern.*, Oct. 2006, pp. 3534–3539, doi: 10.1109/ICSMC.2006.384667.

[16] T. C. Greene, P. A. Bell, and W. N. Boyer, "Coloring the environment: Hue, arousal, and boredom," *Bull. Psychonomic Soc.*, vol. 21, no. 4, pp. 253–254, 1983.

[17] A. G. Schauss, "The physiological effect of color on the suppression of human aggression: Research on Baker-Miller pink," *Int. J. Biosocial Res.*, vol. 7, no. 2, pp. 55–64, 1985.

[18] P. Valdez and A. Mehrabian, "Effects of color on emotions," *J. Exp. Psychol., Gen.*, vol. 123, no. 4, pp. 394–409, 1994.

[19] C.-Y. Wei, N. Dimitrova, and S.-F. Chang, "Color-mood analysis of films based on syntactic and psychological models," in *Proc. IEEE Int. Conf. Multimedia Expo (ICME)*, Taiwan, vol. 2, Jun. 2004, pp. 831–834, doi: 10.1109/ICME.2004.1394329.

[20] G. Meerwein, B. Rodeck, and F. H. Mahnke, *Color-Communication in Architectural Space*, 4th ed. Berlin, Germany: Walter de Gruyter, 2007.

[21] H. J. Suk and H. Irtel, "Emotional response to color across media," *Color Res. Appl.*, vol. 35, no. 1, pp. 64–77, 2010, doi: 10.1002/col.20554.

[22] R. E. Mayer and G. Estrella, "Benefits of emotional design in multimedia instruction," *Learn. Instruct.* vol. 33, pp. 12–18, Oct. 2014, doi: 10.1016/j.learninstruc.2014.02.004.

[23] A. Yoto, T. Katsuura, K. Iwanaga, and Y. Shimomura, "Effects of object color stimuli on human brain activities in perception and attention referred to EEG alpha band response," *J. Physiol. Anthropol.*, vol. 26, no. 3, pp. 373–379, 2007, doi: 10.2114/jpa2.26.373.

[24] L. Wilms and D. Oberfeld, "Color and emotion: Effects of hue, saturation, and brightness," *Psychol. Res.*, vol. 82, no. 5, pp. 896–914, Sep. 2018, doi: 10.1007/s00426-017-0880-8.

[25] A. J. Elliot, "Color and psychological functioning: A review of theoretical and empirical work," *Frontiers Psychol.*, vol. 6, p. 368, Apr. 2015, doi: 10.3389/fpsyg.2015.00368.

[26] K. W. Jacobs and F. E. Hustmyer, "Effects of four psychological primary colors on GSR, heart rate and respiration rate," *Perceptual Motor Skills*, vol. 38, no. 3, pp. 763–766, 1974.

[27] J. Walters, M. J. Apter, and S. Svebak, "Color preference, arousal, and the theory of psychological reversals," *Motivat. Emotion*, vol. 6, no. 3, pp. 193–215, 1982.

[28] P. K. Kaiser, "Physiological response to color: A critical review," *Color Res. Appl.*, vol. 9, no. 1, pp. 29–36, Mar. 1984.

[29] G.V. Tcheslavski, M. Vasefi, and F. F. Gonen, "Response of a human visual system to continuous color variation: An EEG-based approach," *Biomed. Signal Process. Control* vol. 43, pp. 130–137, May 2018, doi: 10.1016/j.bspc.2018.03.001.

[30] Y. Ueda, K. Hayashi, K. Kuroiwa, N. Miyoshi, H. Kashiba, and D. Takeda, "Consciousness and recognition of five colors: Using functional-MRI and brain wave measurements," *J. Int. Soc. Life Inf. Sci.*, vol. 22, no. 2, pp. 366–371, 2004.

[31] World Medical Organization, "Declaration of Helsinki," *Brit. Med. J.*, vol. 313, no. 7070, pp. 1448–1449, 1996. [Online]. Available: http://www.cirp.org/library/ethics/helsink, doi: 10.1016/j.neuroimage.2021.118030.

[32] MathWorks. *MATLAB 2017*. Accessed: Dec. 15, 2022. [Online]. Available: https://www.mathworks.com/

[33] A. Delorme and S. Makeig, "EEGLAB: An open source toolbox for analysis of single-trial EEG dynamics including independent component analysis," *J. Neurosci. Methods*, vol. 134, no. 1, pp. 9–21, 2004.

[34] L. Dong, F. Li, Q. Liu, X. Wen, Y. Lai, P. Xu, and D. Yao, "MATLAB toolboxes for reference electrode standardization technique (REST) of scalp EEG," *Frontiers Neurosci.*, vol. 11, p. 601, Oct. 2017.

[35] J. Sun, B. Sun, B. Wang, and H. Gong, "The processing bias for threatening cues revealed by event-related potential and event-related oscillation analyses," *Neuroscience*, vol. 207, pp. 91–98, Feb. 2012.

[36] H. Nolan, R. Whelan, and R. Reilly, "FASTER: Fully automated statistical thresholding for EEG artifact rejection," *J. Neurosci. Methods*, vol. 192, no. 1, pp. 152–162, 2010.

[37] M. Balconi and U. Pozzoli, "Event-related oscillations (EROs) and event-related potentials (ERPs) comparison in facial expression recognition," *J. Neuropsychol.*, vol. 1, no. 2, pp. 283–294, 2007.

[38] M. Balconi and U. Pozzoli, "Event-related oscillations (ERO) and event-related potentials (ERP) in emotional face recognition: A regression analysis," *Int. J. Neurosci.*, vol. 118, no. 10, pp. 1412–1424, 2008.

[39] C. Andrew and G. Fein, "Event-related oscillations versus event-related potentials in a P300 task as biomarkers for alcoholism," *Alcoholism: Clin. Exp. Res.*, vol. 34, no. 4, pp. 669–680, 2010.

[40] M. X. Cohen, *Analyzing Neural Time Series Data: Theory and Practice*. Cambridge, MA, USA: MIT Press, 2014.

[41] D. M. Groppe, T. P. Urbach, and M. Kutas, "Mass univariate analysis of event-related brain potentials/fields I: A critical tutorial review," *Psychophysiology*, vol. 48, no. 12, pp. 1711–1725, Dec. 2011.

[42] S. J. Luck, *An Introduction to the Event-Related Potential Technique*. MIT Press, 2014. [Online]. Available: https://mitpress.mit.edu/9780262525855/

[43] E. Maris and R. Oostenveld, "Nonparametric statistical testing of EEG-and MEG-data," *J. Neurosci. Methods*, vol. 164, no. 1, pp. 177–190, 2007.

[44] D. Groppe, T. Urbach, and M. Kutas, "Mass univariate analysis of event-related brain potentials/fields II: Simulation studies," *Psychophysiology*, vol. 48, no. 12, pp. 1726–1737, 2011.

[45] W. J. Ray and H. W. Cole, "EEG alpha activity reflects attentional demands, and beta activity reflects emotional and cognitive processes," *Science*, vol. 228, no. 4700, pp. 750–752, May 1985.

[46] B. Güntekin and E. Basar, "Event-related beta oscillations are affected by emotional eliciting stimuli," *Neurosci. Lett.*, vol. 483, no. 3, pp. 173–178, 2010.

[47] V. B. Pavlenko, S. V. Chernyi, and D. G. Goubkina, "EEG correlates of anxiety and emotional stability in adult healthy subjects," *Neurophysiology*, vol. 41, no. 5, pp. 337–345, Oct. 2009.

[48] S. B. Andersen, R. A. Moore, L. Venables, and P. J. Corr, "Electrophysiological correlates of anxious rumination," *Int. J. Psychophysiol.*, vol. 71, pp. 156–169, Feb. 2009.

[49] J. J. Foxe and A. C. Snyder, "The role of alpha-band brain oscillations as a sensory suppression mechanism during selective attention," *Frontiers Psychol.*, vol. 2, no. 154, pp. 1–13, 2011, doi: 10.3389/fpsyg.2011.00154.

[50] W. Klimesch, "Alpha-band oscillations, attention, and controlled access to stored information," *Trends Cogn. Sci.*, vol. 16, no. 12, pp. 606–617, 2012, doi: 10.1016/j.tics.2012.10.007.

[51] K. E. Mathewson, A. Lleras, D. M. Beck, M. Fabiani, T. Ro, and G. Gratton, "Pulsed out of awareness: EEG alpha oscillations represent a pulsed-inhibition of ongoing cortical processing," *Frontiers Psychol.*, vol. 2, no. 99, pp. 1–15, 2011, doi: 10.3389/fpsyg.2011.00099.

[52] D. Schubring and H. T. Schupp, "Affective picture processing: Alpha- and lower beta-band desynchronization reflects emotional arousal," *Psychophysiology*, vol. 56, no. 8, 2019, Art. no. e13386.

[53] B. Güntekin and E. Basar, "Emotional face expressions are differentiated with brain oscillations," *Int. J. Psychophysiol.*, vol. 64, no. 1, pp. 91–100, 2007.

[54] L. I. Aftanas, A. A. Varlamov, S. V. Pavlov, V. P. Makhnev, and N. V. Reva, "Time-dependent cortical asymmetries induced by emotional arousal: EEG analysis of event-related synchronization and desynchronization in individually defined frequency bands," *Int. J. Psychophysiol.*, vol. 44, no. 1, pp. 67–82, 2002, doi: 10.1016/S0167-8760(01)00194-5.

[55] L. I. Aftanas, N. V. Reva, A. A. Varlamov, S. V. Pavlov, and V. P. Makhnev, "Analysis of evoked EEG synchronization and desynchronization in conditions of emotional activation in humans: Temporal and topographic characteristics," *Neurosci. Behav. Physiol.*, vol. 34, no. 8, pp. 859–867, 2004, doi: 10.1023/B:NEAB.0000038139.39812.eb.

[56] A. Uusberg, H. Uibo, K. Kreegipuu, and J. Allik, "EEG alpha and cortical inhibition in affective attention," *Int. J. Psychophysiol.*, vol. 89, no. 1, pp. 26–36, Jul. 2013, doi: 10.1016/j.ijpsycho.2013.04.020.

[57] G. G. Knyazev, A. V. Bocharov, E. A. Levin, A. N. Savostyanov, and J. Y. Slobodskoj-Plusnin, "Anxiety and oscillatory responses to emotional facial expressions," *Brain Res.*, vol. 1227, pp. 174–188, Aug. 2008, doi: 10.1016/j.brainres.2008.06.108.

[58] M. Balconi and G. Mazza, "Brain oscillations and BIS/BAS (behavioral inhibition/activation system) effects on processing masked emotional cues.: ERS/ERD and coherence measures of alpha band," *Int. J. Psychophysiol.*, vol. 74, no. 2, pp. 158–165, 2009, doi: 10.1016/j.ijpsycho.2009.08.006.

[59] A. de Cesarei and M. Codispoti, "Affective modulation of the LPP and α-ERD during picture viewing," *Psychophysiology*, vol. 48, no. 10, pp. 1397–1404, 2011, doi: 10.1111/j.1469-8986.2011.01204.x.

[60] Y. Cui, F. Versace, J. M. Engelmann, J. A. Minnix, J. D. Robinson, C. Y. Lam, and P. M. Cinciripini, "Alpha oscillations in response to affective and cigarette-related stimuli in smokers," *Nicotine Tobacco Res.*, vol. 15, no. 5, pp. 917–924, 2013, doi: 10.1093/ntr/nts209.

[61] M. Otten and K. J. Jonas, "Humiliation as an intense emotional experience: Evidence from the electro-encephalogram," *Social Neurosci.*, vol. 9, no. 1, pp. 23–35, 2014, doi: 10.1080/17470919.2013.855660.

[62] X. Meng, W. Liu, L. Zhang, X. Li, B. Yao, X. Ding, and J. Yang, "EEG oscillation evidences of enhanced susceptibility to emotional stimuli during adolescence," *Frontiers Psychol.*, vol. 7, p. 616, Jan. 2016, doi: 10.3389/fpsyg.2016.00616.

[63] N. Furl, M. Lohse, and F. Pizzorni-Ferrarese, "Low-frequency oscillations employ a general coding of the spatio-temporal similarity of dynamic faces," *NeuroImage*, vol. 157, pp. 486–499, Aug. 2017, doi: 10.1016/j.neuroimage.2017.06.023.

[64] T. R. Schneider, J. F. Hipp, C. Domnick, C. Carl, C. Büchel, and A. K. Engel, "Modulation of neuronal oscillatory activity in the beta- and gamma-band is associated with current individual anxiety levels," *NeuroImage*, vol. 178, pp. 423–434, Sep. 2018, doi: 10.1016/j.neuroimage.2018.05.059.

[65] K. E. Mathewson, M. Fabiani, G. Gratton, D. M. Beck, and A. Lleras, "Rescuing stimuli from invisibility: Inducing a momentary release from visual masking with pre-target entrainment," *Cognition*, vol. 115, no. 1, pp. 186–191, Apr. 2010.

[66] J. Besle, C.A. Schevon, A. D. Mehta, P. Lakatos, R. R. Goodman, G. M. McKhann, R. G. Emerson, and C. E. Schroeder, "Tuning of the human neocortex to the temporal dynamics of attended events," *J. Neurosci.*, vol. 31, no. 9, pp. 3176–3185, 2011.

[67] E. Z. Golumbic, G. B. Cogan, C. E. Schroeder, and D. Poeppel, "Visual input enhances selective speech envelope tracking in auditory cortex at a 'cocktail party,'" *J. Neurosci.*, vol. 33, no. 4, pp. 1417–1426, 2013.

[68] M. Eidelman-Rothman, E. Ben-Simon, D. Freche, A. Keil, T. Hendler, and N. Levit-Binnun, "Sleepless and desynchronized: Impaired inter trial phase coherence of steady-state potentials following sleep deprivation," *NeuroImage*, vol. 202, Nov. 2019, Art. no. 116055, doi: 10.1016/j.neuroimage.2019.116055.

[69] J. Ding, G. Sperling, and R. Srinivasan, "Attentional modulation of SSVEP power depends on the network tagged by the flicker frequency," *Cerebral Cortex*, vol. 16, no. 7, pp. 1016–1029, 2005.

[70] Y. Joon Kim, M. Grabowecky, K. A. Paller, K. Muthu, and S. Suzuki, "Attention induces synchronization-based response gain in steady-state visual evoked potentials," *Nature Neurosci.*, vol. 10, no. 1, pp. 117–125, Jan. 2007.

[71] S. Hanslmayr, W. Klimesch, P. Sauseng, W. Gruber, M. Doppelmayr, R. Freunberger, and T. Pecherstorfer, "Visual discrimination performance is related to decreased alpha amplitude but increased phase locking," *Neurosci. Lett.*, vol. 375, no. 1, pp. 64–68, 2005, doi: 10.1016/j.neulet.2004.10.092.

[72] X. Duart, E. Quiles, F. Suay, N. Chio, E. Garcia, and F. Morant, "Evaluating the effect of stimuli color and frequency on SSVEP," *Sensors*, vol. 21, no. 1, p. 117, 2021, doi: 10.3390/s21010117.

[73] M. Guo, J. Jin, Y. Jiao, X. Wang, and A. Cichockia, "Investigation of visual stimulus with various colors and the layout for the oddball paradigm in evoked related potential-based brain–computer interface," *Frontiers Comput. Neurosci.*, vol. 13, p. 24, Apr. 2019.

[74] X. Liu and K. Hong, "Detection of primary RGB colors projected on a screen using fNIRS," *J. Innov. Opt. Health Sci.*, vol. 10, no. 3, 2017, Art. no. 1750006.

[75] S. Roy, A. Banerjee, C. Roy, S. Nag, S. Sanyal, R. Sengupta, and D. Ghosh, "Brain response to color stimuli: An EEG study with nonlinear approach," *Cogn. Neurodyn.*, vol. 15, pp. 1023–1053, Jul. 2021.

[76] D. G. Duru and M. Alobaidi, "Classification of brain electrophysiological changes in response to colour stimuli," *Phys. Eng. Sci. Med.*, vol. 44, no. 3, pp. 727–743, 2021.

[77] D. Regan, "An effect of stimulus colour on average steady-state potentials evoked in man," *Nature*, vol. 210, no. 5040, pp. 1056–1057, Jun. 1966.

[78] D. W. Sutterer, A. J. Coia, V. Sun, S. K. Shevell, and E. Awh, "Decoding chromaticity and luminance from patterns of EEG activity," *Psychophysiology*, vol. 58, no. 4, 2021, Art. no. e13779.

[79] A. Khadir, M. Maghareh, S. S. Ghamsari, and B. Beigzadeh, "Brain activity characteristics of RGB stimulus: An EEG study," *Sci. Rep.*, vol. 13, p. 18988, Nov. 2023, doi: 10.1038/s41598-023-46450-z.

[80] T. Chauhan, I. Jakovljev, L. Thompson, S. Wuerger, and J. Martinovic, "Decoding of EEG signals reveals non-uniformities in the neural geometry of colour," *NeuroImage*, vol. 268, Mar. 2023, Art. no. 119884.

[81] Z. Lu and G. Sperling, "Black–white asymmetry in visual perception," *J. Vis.*, vol. 12, no. 10, p. 8, 2012.

[82] H. S. Jang, G. M. Gim, S. J. Jeong, and J. S. Kim, "Changes in physiological and psychological conditions of humans to color stimuli of plants," *J. People, Plants, Environ.*, vol. 22, no. 2, pp. 127–143, 2019.

[83] A. J. Elliot and M. A. Maier, "Color and psychological functioning," *Current Directions Psychol. Sci.*, vol. 16, no. 5, pp. 250–254, Oct. 2007.

[84] A. J. Elliot, M. A. Maier, A. C. Moller, R. Friedman, and J. Meinhardt, "Color and psychological functioning: The effect of red on performance attainment," *J. Exp. Psychol., Gen.*, vol. 136, no. 1, p. 154, 2007.

[85] S.f Hosseini and A. Ghabanchi, "What's in a Color? A neuropsycholinguistic study on the effect of colors on EEG brainwaves, immediate emotional responses, and English language vocabulary retention among Iranian young adults," *J. Neurolinguistics*, vol. 63, Aug. 2022, Art. no. 101083.

[86] S. Kalantari, V. Tripathi, J. Kan, J. D. Rounds, A. Mostafavi, R. Snell, and J. G. Cruz-Garza, "Evaluating the impacts of color, graphics, and architectural features on wayfinding in healthcare settings using EEG data and virtual response testing," *J. Environ. Psychol.*, vol. 79, Feb. 2022, Art. no. 101744.

[87] M. Lee, C. Kim, B. Sarmandakh, G. Cho, and E. Yi, "Electroencephalogram and psychological response to fragrance and color of citrus unshiu scent-infused fabrics," *Fibers Polym.*, vol. 19, pp. 1548–1555, Aug. 2018.

[88] A. Hassani, A. Hekmatmanesh, and A. M. Nasrabadi, "Gender differences in EEG responses to color and black-white images: Implications for neuromarketing strategies," *IEEE Access*, vol. 11, pp. 93739–93753, 2023, doi: 10.1109/ACCESS.2023.3308810.

ALIREZA KHADIR received the B.Sc. degree in industrial engineering from the Sharif University of Technology, in 2012, and the M.Sc. degree in biomedical engineering from Iran University of Science and Technology, in 2014, where he is currently pursuing the Ph.D. degree in biomedical engineering. His current research interests include cognitive neuroscience, bio-signal processing, and feature binding in visual-working-memory.

BORHAN BEIGZADEH received the B.Sc. degree in mechanical engineering from the University of Tehran, in 2003, and the M.Sc. and Ph.D. degrees in mechanical engineering from the Sharif University of Technology, in 2005 and 2011, respectively. Then, he joined Iran University of Science and Technology, Tehran, Iran, where he is currently an Associate Professor with the School of Mechanical Engineering and established the Biomechatronics and Cognitive Engineering Research Laboratory. His current research interests include non-linear dynamics and control, robotics, biomechatronics, and cognitive engineering.

• • •